Journal of Solid State Chemistry 297 (2021) 122038

Contents lists available at ScienceDirect

Journal of Solid State Chemistry

journal homepage: www.elsevier.com/locate/jssc

Different mechanism of stereochemical activity and birefringence in post-transition metal halides: A first-principles investigation

Kui Wang [a], Qun Jing [a,*], Zhenzhen Wan [a], Ming-Hsien Lee [b], Haiming Duan [a], Haibin Cao [c], Jun Zhang [a,**]

[a] School of Physical Science and Technology, Xinjiang University, 666 Shengli Road, Urumqi, 830046, China
[b] Department of Physics, Tamkang University, New Taipei City, 25137, Taiwan
[c] Department of Physics, College of Sciences, Shihezi University, Shihezi, 832000, China

ARTICLE INFO

Keywords:
A first-principles investigation
Birefringence
Lone-pair
Post-transition metal halides

ABSTRACT

The post-transition metal cations are widely used in rechargeable batteries, solar-cells, and birefringent compounds. In this paper, the electronic structures and birefringence of ternary $CsSnX_3$ (X = Cl, I), $CsPbX_3$ (X = Cl, Br, I), and binary MX_2 (M = Sn, Pb; X = Cl, Br) compounds are investigated using the first-principles methods. The results show that these metal halides own different mechanism in stereochemical activity and birefringence, i.e., the stereochemical activity of lone-pair electrons are determined by energy difference between cation s states and halogen p states, and the stereochemical activity decreases from Cl to I. While the cation p states play an important role in determining the birefringence, and the birefringence increased from Cl to I.

1. Introduction

Nonlinear optical (NLO) materials have potential application in optical information processing [1–3], photolithography, precise micromachining, and so on [4–6]. During the past decades, hundreds of novel NLO compounds have been invented, including commercially widely used β-BaB_2O_4 (BBO) [7], LiB_3O_5(LBO) [8], CsB_3O_5 (CBO) [9], $CsLiB_6O_{10}$ (CLBO) [10,11], $KBe_2(BO_3)F_2$(KBBF) [12]and lots of borates [13] and fluorooxoborates [4,5,14–22], carbonates [23–25], phosphates [26–29]. Generally speaking, excellent nonlinear materials should have suitable band gap, birefringence, and large SHG response [5]. Hence kinds of functional chromophores, like anionic groups, d^0 or d^{10} transition metal cations [30,31], post-transition metal cations containing stereochemically active lone pair electrons [32–36], were introduced to get enhanced response [37].

Post-transition metal cations, locating at the bottom of Group 13, 14, and 15, like Pb(II) and Sn(II), are widely used in rechargeable batteries [38], solar cells [39–42], and nonlinear optical (NLO) compounds [28,29,43–49]. The stereochemically active lone-pair electrons are beneficial to get enhanced birefringence and/or second-harmonic generation (SHG) response. For example, $Pb_2B_5O_9I$ compound owns relative large SHG response as 13.5 times that of KDP [32], Pb_2BO_3X(X = Cl, Br, and I) own SHG response as 9 × , 9.5 × , and 10 × KDP, respectively [33–35]. The birefringence of $BaSn_2(PO_4)_2$ is reported as 0.071@1064 nm [50], the birefringence of $Sn_2B_5O_9Cl$ is reported as 0.168@546 nm [51]. Using the first-principles method, Wash et al. pointed out that the interaction of cation p states and cation s-O p states results in asymmetric lone-pair electron distribution [38,52–55]. The asymmetric lone-pair electrons can help metal oxides get enhanced birefringence or SHG response [56–59].

Excepting metal oxides, metal halides can also give relatively large birefringence and/or SHG response. Recently, Guo et al. reported that the birefringence of $PbCl_2$, $SbCl_3$, and α-SnF_2 are 0.046, 0.172, and 0.177, respectively [44]. As for ternary metal halides, a series of perovskite ABX_3 (A = Cs, Rb; B= Ge, Cd; X = Cl, Br, I) [60–66] have been reported. While to best of our knowledge, there is still no reports about the electronic structures and birefringence of these perovskite ABX_3. In this paper, the electronic structures and optical properties of ternary $CsSnX_3$ (X = Cl, I), $CsPbX_3$ (X = Cl, Br, I) compounds and binary MX_2 (M = Sn, Pb; X = Cl, Br) compounds have been investigated using the first-principles methods. For Sn(II) (or Pb(II)) compounds, the asymmetric lone-pair electronic distribution gradually decreased from Cl to I, while birefringence gradually increased. The results show that energy difference of cations-s and halogens-p states play an important role in the

* Corresponding author.
** Corresponding author.
E-mail addresses: qunjing@xju.edu.cn (Q. Jing), zhj@xju.edu.cn (J. Zhang).

https://doi.org/10.1016/j.jssc.2021.122038
Received 4 December 2020; Received in revised form 19 January 2021; Accepted 30 January 2021
Available online 5 February 2021

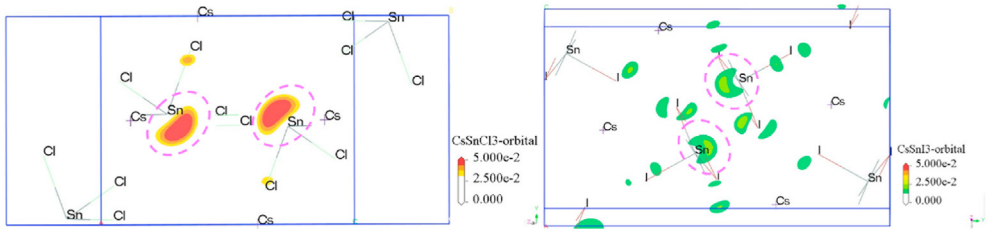

Fig. 1. The orbital cross-sectional diagrams of $CsSnCl_3$(left) and $CsSnI_3$(right) compounds near the Fermi surface.

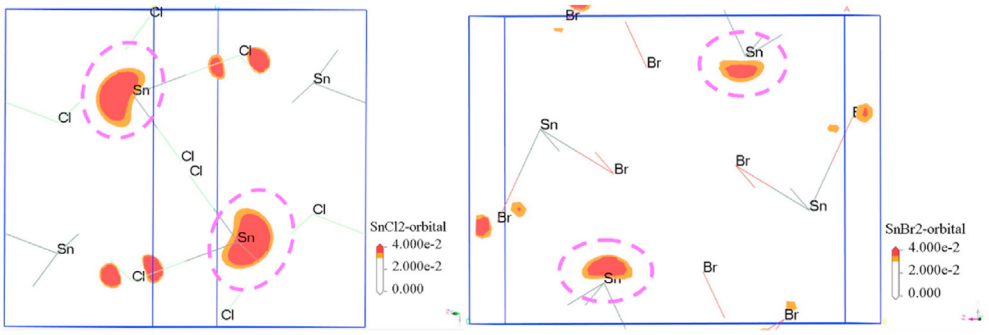

Fig. 2. The orbital cross-sectional diagrams of SnX_2 (X = Cl, Br) compounds near the Fermi surface.

lone pair effect, and the birefringence have closely relationship with p orbital of cations.

2. Numerical calculations details

In this paper, the electronic structures and optical properties of the ternary $CsSnX_3$ (X = Cl, I), $CsPbX_3$ (X = Cl, Br, I), and binary MX_2 (M = Sn, Pb; X = Cl, Br) compounds were calculated using the CASTEP software package based on the first-principles methods [67]. The generalized gradient approximation (GGA) using the Perdew–Burke–Ernzerhof (PBE) functional [68,69] and the norm-conserving pseudopotentials (NCPs) [70] were adopted. For these compounds, the following valence electron configurations were used: $Cs(5s^25p^66s^1)$, $Sn(5s^25p^2)$, $Pb(5s^25p^65d^{10}6s^26p^2)$, $Cl(3s^23p^5)$, $Br(4s^24p^5)$, $I(5s^25p^5)$. The cut-off value of kinetic energy were set to 830 eV($CsSnCl_3$), 440 eV($CsSnI_3$), 910 eV($CsPbX_3$), 830 eV($SnCl_2$), 280

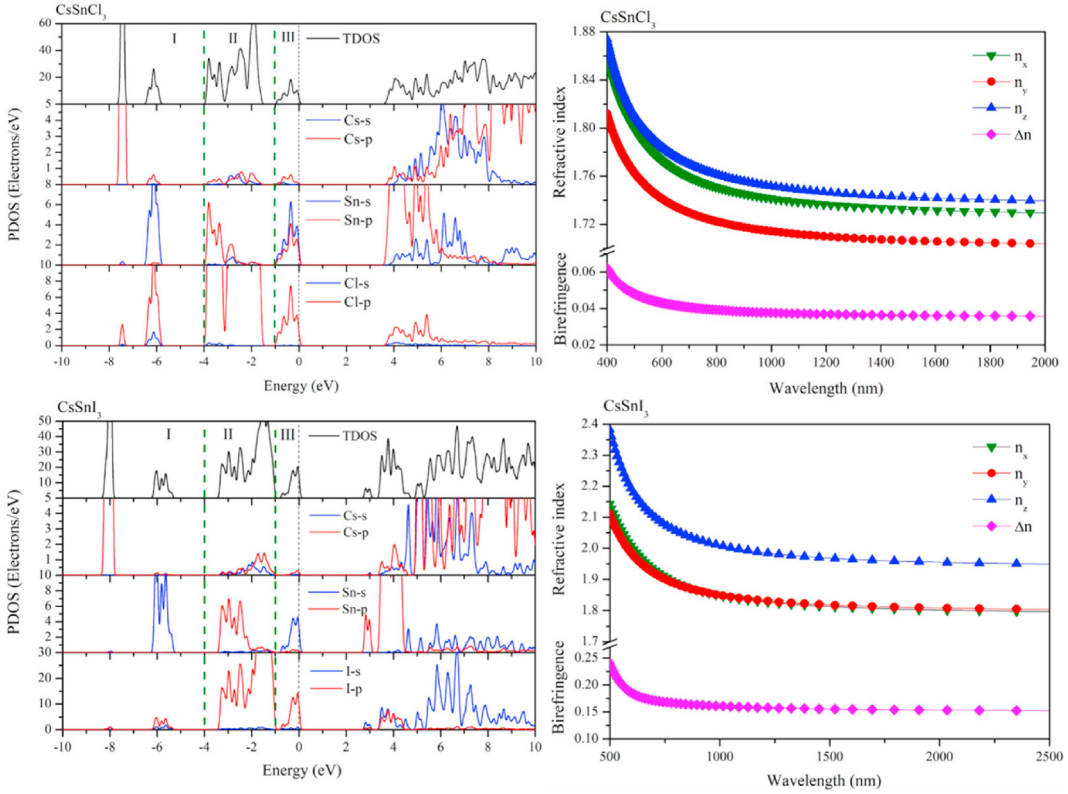

Fig. 3. The PDOS (projected density of states) and birefringence of $CsSnX_3$ (X = Cl, I) obtained using PBE functional.

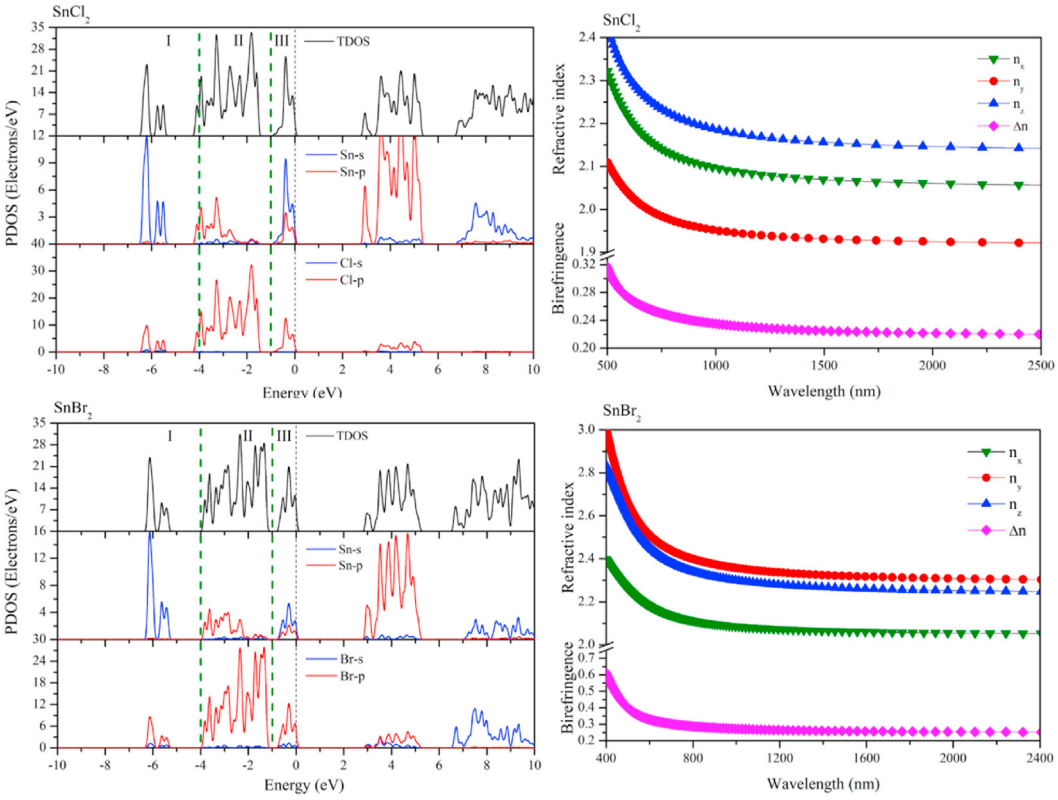

Fig. 4. The PDOS (projected density of states) and birefringence of SnX_2 (X = Cl, Br) obtained using PBE functional.

eV($SnBr_2$), and 910 eV(PbX_2), with the span of the Brillouin zone were selected as 0.04 $Å^{-1}$ and the Monkhorst-Pack k points were 2 × 3 × 4($CsSnCl_3$), 2 × 1 × 5($CsSnI_3$), 3 × 3 × 2($CsPbX_3$), 3 × 3 × 6($SnCl_2$), 3 × 6 × 2($SnBr_2$), 3 × 6 × 3($PbCl_2$), and 3 × 5 × 3($PbBr_2$). Based on the results obtained by GGA-PBE calculation, the refractive indices were examined via calculating the dielectric function $\varepsilon(\omega) = \varepsilon_1(\omega) + i\varepsilon_2(\omega)$, where $\varepsilon_1(\omega)$ and $\varepsilon_2(\omega)$ are the real and imaginary part of dielectric function, respectively. More details about how to calculate $\varepsilon_1(\omega)$ and $\varepsilon_2(\omega)$ are shown in SI. Herein, the scissors, defined as the bandgap difference between the HSE06 and GGA-PBE, were used to get the refractive indices.The HSE06 functional [71–73] implemented in the PWMAT [74,75] package was also chosen to get reliable bandgap comparable with experimental value [13], [59,76,77]. During the PWMAT-HSE06 calculation, the Monkhorst-pack k points were set as CASTEP-PBE calculation, and the cutoff energies were set as 816 eV.

3. Result and conclusion

3.1. The asymmetric lone-pair electronic distribution

The asymmetric lone-pair electronic distribution of ternary compounds $CsSnCl_3$, $CsSnI_3$, $CsPbX_3$ (X = Cl, Br, I), and binary compounds MX_2 (M = Sn, Pb; X = Cl, Br) were firstly determined using the orbitals nearby the Fermi level. The obtained orbitals of these compounds are shown in Figs. 1 and 2, and Figs. S4-S5. Take $CsSnX_3$ (X = Cl, and I) for example. As shown in Fig. 1, there are obvious semicircular or lobe-shaped electron clouds around Sn atoms, indicating asymmetric lone-pair electronic distribution can be found around Sn(II) cations. Like $CsSnX_3$ (X = Cl and I) compounds, the asymmetric lone-pair electronic distribution can also be found around Sn(II) cations in SnX_2 (X = Cl, Br) compounds (shown in Fig. 2). While unlike $CsSnX_3$ (X = Cl, and I) and SnX_2 (X = Cl, Br) compounds, the asymmetric lone-pair electronic distribution around Pb(II) cations in $CsPbX_3$ (X = Cl, Br, and I) and PbX_2 (X = Cl, Br) compounds are inconspicuous. As shown in Fig. S4 and Fig. S5, there were elliptical electrons around Pb(II) cations.

To deeply understanding the origination of the different electron distribution around Sn(II)/Pb(II) cations, the band structures (described in SI) and projected density of states (PDOS) of these compounds are also obtained. According to the revised model of metal oxides suggested by Walsh et al. [52], the authors would pay more attention to the states about Sn(II)/Pb(II) and halogens locating at the top of the valence band. As shown in Figs. 3 and 4, according to the interaction between Sn(II) and halogens, the states at the top of valence band can be divided into three different energy region. Take $CsSnCl_3$ for example. At the region I whose energy below −4 eV, there are mainly Sn-s states and Cl-p states (around −6 eV), indicating the hybrid Sn s-Cl p states are found in this region. For the region II, there are mainly Sn-p states, Cl-p states, and few Sn-s states. As for region III nearby the Fermi level, there are mainly Sn-s states, Cl-p states and relatively few Sn-p states. The states locating in region III should be the Sn p-(Sn s-Cl p)* states, which shows asymmetric lone-pair distribution (shown in Fig. 1). Similar conclusion can also be found in $CsSnI_3$, and binary compounds SnX_2 (X = Cl, Br, shown in Figs. 3 and 4). While unlike $CsSnX_3$ and SnX_2 compounds, more Pb-p states are found in region III of $CsPbX_3$ and PbX_2 compounds (shown in Fig. 5 and Fig. 6), which would weaken the stereochemical activity of lone pair electronic distribution around Pb(II) cations (shown in Fig. S4 and Fig. S5).

For metal oxides, Walsh et al. pointed out that the energy separation between cations-s and O-2p plays an important role in determining the stereo-chemical activity of the lone pair, that's the smaller the energy separation is, the stronger the stereochemically activity has. Hence in metal oxides, the post-transition metal owns the sequence of stereo-chemical activity of lone pair as: Sn > Pb > Sb > Bi > Te > Po [52]. Herein, the authors have recalculated the atomic energy of Pb, Sn and halogens using B3LYP [78,79]/(ECP)LanL2DZ [80] level with Gaussian 09 software package [81]. The obtained atomic orbital energy and the energy difference between different states are shown in Fig. 7.

As shown in Fig. 7, one can immediately find that, for given halogens, the energy difference between tin and halogens is smaller than that of

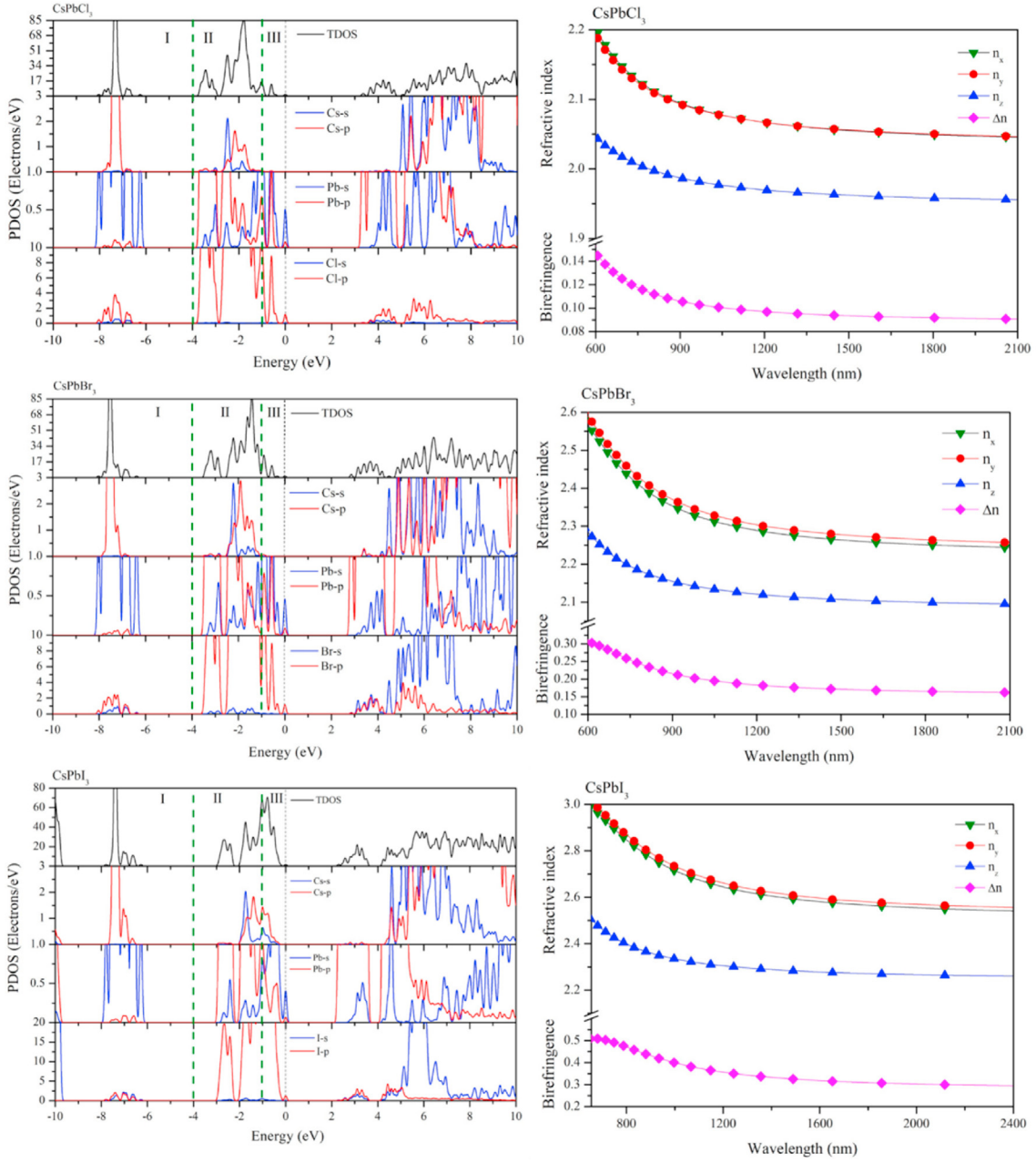

Fig. 5. The PDOS (projected density of states) and birefringence of $CsPbX_3$ (X = Cl, Br, I) obtained using PBE functional.

lead and halogens. For example, the energy difference of Pb–Cl is 3.12 eV, while the energy difference of Sn–Cl is 1.44 eV. According to the revised model suggested by Walsh et al., the smaller energy difference is beneficial to get stronger chemical activity of asymmetric lone pair electron distribution. That's why obvious lobe-like electronic distribution can be found around Sn(II) cations. Similarly, for given cations, the energy difference between Sn(II) (or Pb(II)) cation and halogens gradually increased from Cl to I, so the stereochemical activity of asymmetric lone-pair electrons gradually decreased (shown in Figs. 1 and 2, and Figs. S4-S5).

3.2. The relationship between birefringence and p states

Using the methods described above, the refractive indices and birefringence of these ternary compounds are also obtained (shown in Figs. 3–6). The obtained birefringence of $CsSnCl_3$ and $CsSnI_3$ are 0.037 and 0.160@1064 nm. The birefringence of $CsPbX_3$ (X = Cl, Br, I) were 0.101, 0.195, and 0.382, respectively. One can immediately find out that the birefringence of these compounds is gradually increased from Cl to I. Similar conclusions can also be found in binary metal halides SnX_2 and PbX_2. The birefringence of $SnCl_2$, $SnBr_2$, $PbCl_2$, and $PbBr_2$ were 0.188, 0.269, 0.030, and 0.119 (in Figs. 4 and 6). The calculated birefringence of $PbCl_2$ is slightly smaller than the experimental value [44]. Noting that as described above, the stereochemical activity of lone pair electronic distribution gradually decreased from Cl to I. As described elsewhere [50,56,82], the lone-pair electronic distribution is beneficial to get enhanced birefringence. Curiously, how can different trend be found in stereochemical activity and birefringence of these post-transition metal halides?

It is well known that the optical properties have relation with the electron transition among the states nearby the Fermi level. Hence let us go back to the states at the bottom of conduction band and the top of valence band. For $CsSnX_3$ (X = Cl, I), the top of the valence band are mainly the hybrid Sn-s and X-p orbitals with few Sn-p orbitals, and the

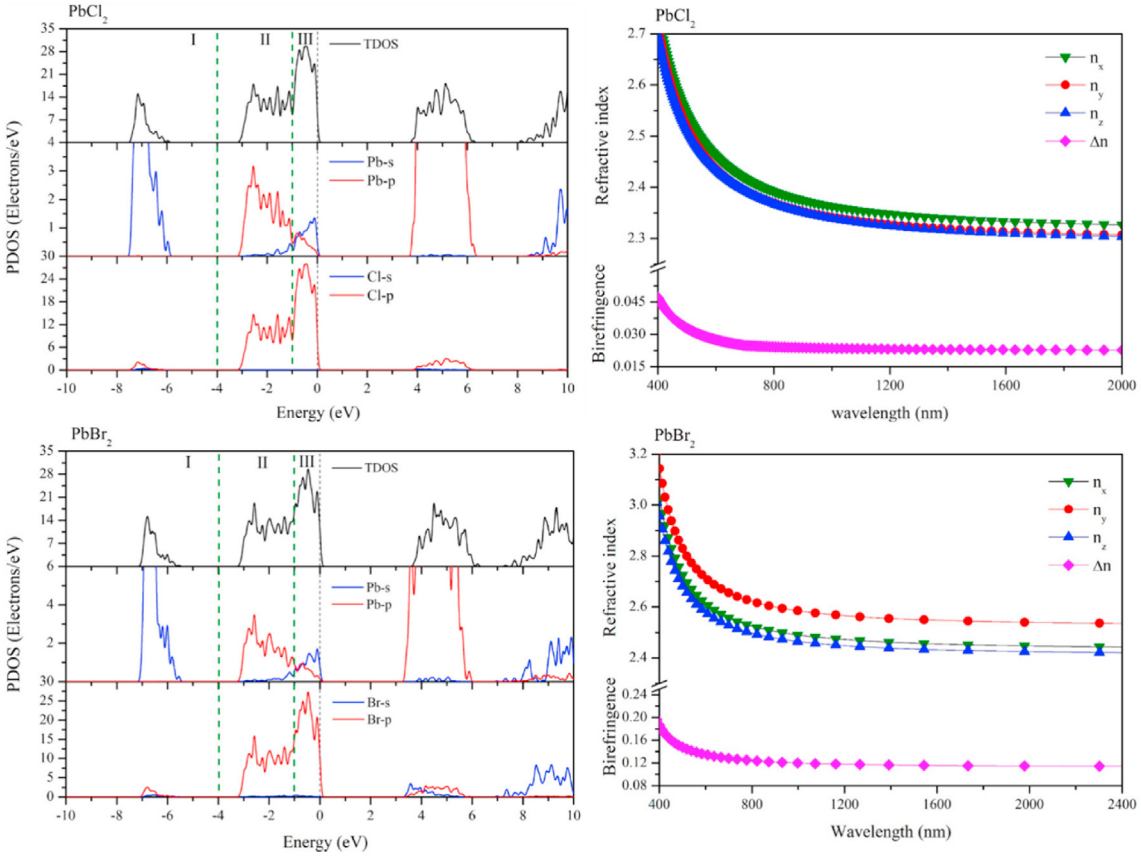

Fig. 6. The PDOS (projected density of states) and birefringence of PbX_2 (X = Cl, Br) obtained using PBE functional.

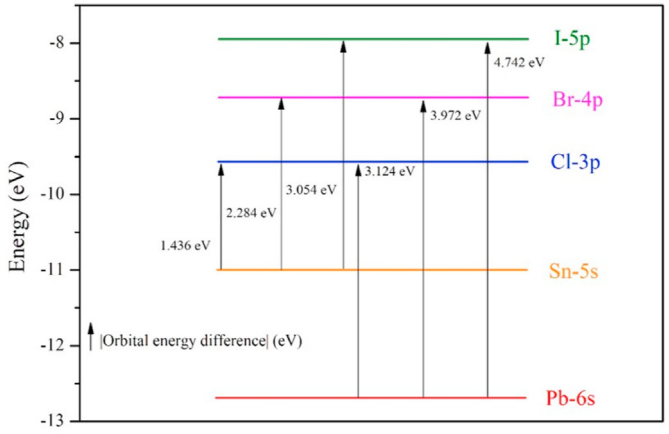

Fig. 7. The obtained absolute value of Energy level difference between halogen and Sn/Pb atom.

bottom of conduction band are mainly Sn-p states; implying the Sn-p states would play an important role in determining the optical properties. Similar conclusions can also be found in other post-transition metal halides. For $CsPbX_3$ (X = Cl, Br, I), the top of the valence band is mainly the Pb-sp and X-p orbitals, and the bottom of the conduction band are mainly the Pb-p orbitals. For the MX_2 (M = Sn, Pb; X = Cl, Br), the cation-p states also give contribution to the optical transition near the Fermi surface. In a word, the authors believe that the cation-p states would play an important role in determining the refractive indices and birefringence [56]. Hereafter, the authors would give a quantitative description using the formula like R(M-p) = S(M-p)/[S(M-s) + S(M-p) + S(X-p)] (S is the integral area of corresponding states at the top of valence band, M are Sn/Pb cations, and X are halogens). Electron transitions coming from the deep energy give minor contribution to the optical properties of compounds, so the energy smaller than −10 eV were omitted. The obtained ratio of M-p (M are Sn(II) and Pb(II) cations) are shown in Fig. 8.

As shown in Fig. 8, for ternary $CsPbX_3$ (X = Cl, Br, and I) and $CsSnX_3$(X = Cl, and I) compounds, the ratio of Pb-p(Sn-p) states own similar tendency like birefringence, that's they all increase from Cl to I. Similar conclusion can also be found in binary PbX_2 (X = Cl, Br) and SnX_2 (X = Cl, Br) compounds (shown in right part of Fig. 8). While according to the revised model suggested by Walsh et al. (as described in section 3.1), the stereochemical activity of lone-pair electrons has relation with energy difference between cation-s and halogen-p states. The authors also calculate the ratio of Pb-s(Sn-s) using the formula as R(M-s) = S(M-s)/[S(M-s) + S(M-p) + S(X-p)] (S is the integral area of corresponding states at the top of valence band, M are Sn/Pb cations, and X are halogens). The obtained ratio of Pb-s(Sn-s) are also shown in Fig. 8. As shown in Fig. 8, the ratio of Pb-s(Sn-s) is disordered, unlike the stereochemical activity of lone-pair electron distribution and birefringence. In a word, for post-transition metal halides discussed in this paper, the stereochemical activity of lone-pair electrons are determined by energy difference between cation s states and halogen p states, and the stereochemical activity decreases from Cl to I. While the cation p states play an important role in determining the birefringence, and the birefringence increased from Cl to I.

4. Conclusions

In this paper, the electronic structures and optical properties of the ternary $CsPbX_3$ (X = Cl, Br, I), $CsSnX_3$ (X = Cl, I), and binary MX_2 (M = Sn, Pb; X = Cl, Br) are detailed investigated using the first-principles methods. The results show that for these post-transition metal halides, the stereochemical activity of Sn(II) cations is stronger than Pb(II) cations. For post-transition metal halides discussed in this paper, the

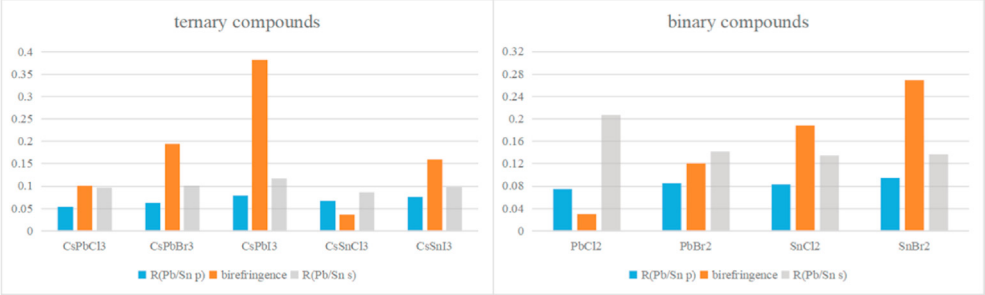

Fig. 8. The obtained birefringence, *R*(Pb/Sn s), *R*(Pb/Sn p) of ternary and binary compounds.

stereochemical activity of lone-pair electrons are determined by energy difference between cation s states and halogen p states, and the stereochemical activity decreases from Cl to I. While the cation p states play an important role in determining the birefringence, and the birefringence increased from Cl to I. The obtained conclusions can help to design enhanced birefringent metal halides.

CRediT authorship contribution statement

Kui Wang: Software, Validation, Formal analysis, Investigation, Writing - original draft. **Qun Jing:** Conceptualization, Software, Writing - review & editing, Supervision, Funding acquisition. **Zhenzhen Wan:** Software, Validation. **Ming-Hsien Lee:** Methodology. **Haiming Duan:** Resources, Methodology. **Haibin Cao:** Resources. **Jun Zhang:** Project administration.

Declaration of competing interest

The authors declare that they have no known competing financial interests or personal relationships that could have appeared to influence the work reported in this paper.

Acknowledgements

This work is supported by the National Natural Science Foundation of China (Grant No. 11864040), the National Undergraduate Training Program for Innovation (Grant No. 202010755012), the Natural Science Foundation of Xinjiang Uygur Autonomous Region of China (Grant No. 2018D01C072), the Science and Technology Research Program for Colleges and Universities in the Department of Education in Xinjiang Uygur Autonomous Region of China (Grant No. XJEDU2017M006).

Appendix A. Supplementary data

Supplementary data to this article can be found online at https://doi.org/10.1016/j.jssc.2021.122038.

References

[1] B. Deepa, P. Philominathan, Optik 127 (2016) 1507–1510.
[2] H. Yu, W. Zhang, P.S. Halasyamani, Cryst. Growth Des. 16 (2016) 1081–1087.
[3] C. Chen, T. Sasaki, R. Li, Y. Wu, Z. Lin, Y. Mori, Z. Hu, J. Wang, S. Uda, M. Yoshimura, Y. Kaneda, Discrete Math. 26 (2012) 43–50.
[4] M. Mutailipu, S. Pan, Angew. Chem. Int. Ed. 59 (2020) 20302–20317.
[5] M. Mutailipu, M. Zhang, Z. Yang, S. Pan, Acc. Chem. Res. 52 (2019) 791–801.
[6] H. Yu, J. Young, H. Wu, W. Zhang, J.M. Rondinelli, S. Halasyamani, Adv. Opt. Mater. 5 (2017) 1700840.
[7] C. Chen, W. Bochard, J. Aidong, Sci. Sin B 28 (1985) 235–243.
[8] C. Chen, Y. Wu, A. Jiang, B. Wu, G. You, R. Li, S. Lin, J. Opt. Soc. Am. B 6 (1989) 616–621.
[9] Y. Wu, T. Sasaki, S. Nakai, A. Yokotani, H. Tang, C. Chen, Appl. Phys. Lett. 62 (1993) 2614–2615.
[10] Y. Mori, S. Nakajima, A. Miyamoto, M. Inagaki, S. Nakai, Proceedings 2633 (1995) 299–307.
[11] J.M. Tu, D.A. Keszler, Mater. Res. Bull. 30 (1995) 209–215.
[12] C. Chen, G.L. Wang, X.Y. Xu, Appl. Phys. B 97 (2009) 9–25.
[13] H. Wu, S. Pan, K.R. Poeppelmeier, H. Li, D. Jia, Z. Chen, X. Fan, Y. Yang, J.M. Rondinelli, H. Luo, J. Am. Chem. Soc. 133 (2011) 7786–7790.
[14] B. Zhang, G. Shi, Z. Yang, F. Zhang, S. Pan, Angew. Chem. Int. Ed. 56 (2017) 3916–3919.
[15] M. Mutailipu, M. Zhang, B. Zhang, L. Wang, Z. Yang, X. Zhou, S. Pan, Angew. Chem. Int. Ed. 57 (2018) 6095–6099.
[16] X. Wang, Y. Wang, B. Zhang, F. Zhang, S. Pan, Angew. Chem. Int. Ed. 56 (2017) 14119–14123.
[17] M. Mutailipu, M. Zhang, H. Wu, Z. Yang, Y. Shen, J. Sun, S. Pan, Nat. Commun. 9 (2018) 3089.
[18] H. Wu, H. Yu, Z. Yang, X. Hou, X. Su, S. Pan, K.R. Poeppelmeier, J.M. Rondinelli, J. Am. Chem. Soc. 135 (2013) 4215–4218.
[19] G.Q. Shi, Y. Wang, F.F. Zhan, B.B. Zhang, R.H. Yang, X.L. Hou, S.L. Pan, K.R. Poeppelmeier, J. Am. Chem. Soc. 139 (2017) 10645–10648.
[20] X. Wang, Y. Wang, B. Zhang, F. Zhang, Z. Yang, S. Pan, Angew. Chem. Int. Ed. 56 (2017) 14119–14123.
[21] M. Mutailipu, M. Zhang, B. Zhang, L. Wang, Z. Yang, X. Zhou, S. Pan, Angew. Chem. Int. Ed. Engl. 57 (2018) 6095–6099.
[22] Y. Wang, B. Zhang, Z. Yang, S. Pan, Angew. Chem. Int. Ed. 57 (2018) 2150–2154.
[23] G. Zou, N. Ye, L. Huang, X. Lin, J. Am. Chem. Soc. 133 (2011) 20001–20007.
[24] G. Zou, L. Huang, N. Ye, C. Lin, W. Cheng, H. Huang, J. Am. Chem. Soc. 135 (2013) 18560–18566.
[25] W. Zhang, P.S. Halasyamani, CrystEngComm 19 (2017) 4742–4748.
[26] J. Lu, J.N. Yue, L. Xiong, W.K. Zhang, L. Chen, L.M. Wu, J. Am. Chem. Soc. 141 (2019) 8093–8097.
[27] J. Chen, L. Xiong, L. Chen, L.M. Wu, J. Am. Chem. Soc. 140 (2018) 14082–14086.
[28] L. Qi, Z. Chen, X. Shi, X. Zhang, Q. Jing, N. Li, Z. Jiang, B. Zhang, M.-H. Lee, Chem. Mater. 32 (2020) 8713–8723.
[29] X. Lu, Z. Chen, X. Shi, Q. Jing, M.H. Lee, Angew. Chem. Int. Ed. Engl. 132 (2020) 17801–17809.
[30] H. Yu, M.L. Nisbet, K.R. Poeppelmeier, J. Am. Chem. Soc. 140 (2018) 8868–8876.
[31] W.L. Zhang, W.D. Cheng, H. Zhang, L. Geng, C.S. Lin, Z.Z. He, J. Am. Chem. Soc. 132 (2010) 1508–1509.
[32] Y.Z. Huang, L.M. Wu, X.T. Wu, L.H. Li, L. Chen, Y.F. Zhang, J. Am. Chem. Soc. 132 (2010) 12788–12789.
[33] H. Yu, N.Z. Koocher, J.M. Rondinelli, P.S. Halasyamani, Angew. Chem. Int. Ed. Engl. 57 (2018) 6100–6103.
[34] G. Zou, C. Lin, H. Jo, G. Nam, T.S. You, K.M. Ok, Angew. Chem. Int. Ed. Engl. 55 (2016) 12078–12082.
[35] M. Luo, Y. Song, F. Liang, N. Ye, Z. Lin, Inorg. Chem. Front. 5 (2018) 916–921.
[36] W. Zhao, S. Pan, J. Han, J. Yao, Y. Yang, J. Li, M. Zhang, L.H. Zhang, Y. Hang, J. Solid State Chem. 184 (2011) 2849–2853.
[37] G. Zou, K.M. Ok, Chem. Sci. 11 (2020) 5404–5409.
[38] A. Walsh, G.W. Watson, Phys. Rev. B 70 (2004) 235114.
[39] J. Brgoch, A.J. Lehner, M. Chabinyc, R. Seshadri, J. Phys. Chem. C 118 (2014) 27721–27727.
[40] L. Lang, J.-H. Yang, H.-R. Liu, H.J. Xiang, X.G. Gong, Phys. Lett. 378 (2014) 290–293.
[41] A.J. Lehner, D.H. Fabini, H.A. Evans, C.-A. Hébert, S.R. Smock, J. Hu, H. Wang, J.W. Zwanziger, M.L. Chabinyc, R. Seshadri, Chem. Mater. 27 (2015) 7137–7148.
[42] J. Qian, B. Xu, W. Tian, Org. Electron. 37 (2016) 61–73.
[43] J.M. Rondinelli, E. Kioupakis, Res. 45 (2015) 491–518.
[44] J. Guo, A. Tudi, S. Han, Z. Yang, S. Pan, Angew. Chem. Int. Ed. Engl. 59 (2020), https://doi.org/10.1002/anie.202014279.
[45] X. Chen, H. Jo, K.M. Ok, Angew. Chem. Int. Ed. 59 (2020) 7514–7520.
[46] X. Chen, Q. Jing, K.M. Ok, Angew. Chem. Int. Ed. 59 (2020) 20323–20327.
[47] H. Zhang, M. Zhang, S. Pan, X. Dong, Z. Yang, X. Hou, Z. Wang, K.B. Chang, K.R. Poeppelmeier, J. Am. Chem. Soc. 137 (2015) 8360–8363.
[48] W.Q. Chen, Q. Jing, Q.Q. Zhang, M.H. Lee, X.F. Lu, P. Wei, Z.H. Chen, Eur. J. Inorg. Chem. (2019) 1273–1278.
[49] H. Yu, H. Wu, Q. Jing, Z. Yang, P.S. Halasyamani, S. Pan, Chem. Mater. 27 (2015) 4779–4788.
[50] Y. Yang, Y. Qiu, P. Gong, L. Kang, G. Song, X. Liu, J. Sun, Z. Lin, Chemistry 25 (2019) 5648–5651.
[51] J. Guo, A. Tudi, S. Han, Z. Yang, S. Pan, Angew. Chem. Int. Ed. Engl. 58 (2019) 17675–17678.
[52] A. Walsh, D.J. Payne, R.G. Egdell, G.W. Watson, Chem. Soc. Rev. 40 (2011) 4455–4463.

[53] A. Walsh, G.W. Watson, J. Solid State Chem. 178 (2005) 1422–1428.
[54] D.J. Payne, R.G. Egdell, A. Walsh, G.W. Watson, J. Guo, P.A. Glans, T. Learmonth, K.E. Smith, Phys. Rev. Lett. 96 (2006) 157403.
[55] A. Walsh, G.W. Watson, J. Phys. Chem. B 109 (2005) 18868–18875.
[56] Q. Jing, Z. Yang, S. Pan, D. Xue, Phys. Chem. Chem. Phys. 17 (2015) 21968–21973.
[57] Q. Jing, X. Dong, Z. Yang, S. Pan, Dalton Trans. 44 (2015) 16818–16823.
[58] X. Dong, Q. Jing, Y. Shi, Z. Yang, S. Pan, K.R. Poeppelmeier, J. Young, J.M. Rondinelli, J. Am. Chem. Soc. 137 (2015) 9417–9422.
[59] X. Shi, Q. Jing, Z. Chen, M.-H. Lee, H. Duan, H. Ding, J. Appl. Phys. 128 (2020).
[60] Q. Zhang, H. Mushahali, H. Duan, M.-H. Lee, Q. Jing, Optik 179 (2019) 89–98.
[61] Q.T. Gu, C.S. Fang, W. Shi, X.W. Wu, Q.W. Pan, J. Cryst. Growth 225 (2001) 501–504.
[62] L.C. Tang, J.Y. Huang, C.S. Chang, M.H. Lee, L.Q. Liu, J. Phys. Condens. Matter 17 (2005) 7275–7286.
[63] G.Z. Lin, C.L. Tang, C. P. Chou Chou, J. Cryst. Growth 47 (2008) 2362–2367.
[64] Z.G. Lin, L.C. Tang, C.P. Chou, Inorg. Chem. 39 (2008) 2362–2367.
[65] G. Walters, E.H. Sargent, J. Phys. Chem. Lett. 9 (2018) 1018–1027.
[66] Z.G. Lin, L.C. Tang, C.P. Chou, Opt. Mater. 31 (2009) 28–34.
[67] S.J. Clark, M.D. Segall, C.J. Pickard, P.J. Hasnip, M.J. Probert, K. Refson, M.C. Payne, Z. für Kristallogr. - Cryst. Mater. 220 (2005) 567–570.
[68] M. Ernzerhof, G.E. Scuseria, J. Chem. Phys. 110 (1999) 5029–5036.
[69] J.P. Perdew, K. Burke, M. Ernzerhof, Phys. Rev. Lett. 777 (1996) 3865–3868.
[70] D.R. Hamann, Phys. Rev. B 88 (2013), 085117.
[71] J. Heyd, G.E. Scuseria, J. Phys. Chem. 120 (2004) 7274–7280.
[72] J. Paier, M. Marsman, K. Hummer, G. Kresse, I.C. Gerber, J.G. Ángyán, J. Chem. Phys. 124 (2006) 154709.
[73] A.V. Krukau, O.A. Vydrov, A.F. Izmaylov, G.E. Scuseria, J. Chem. Phys. 125 (2006) 224106.
[74] W. Jia, Z. Cao, L. Wang, J. Fu, X. Chi, W. Gao, L.W. Wang, Comput. Phys. Commun. 184 (2013) 9–18.
[75] W. Jia, J. Fu, Z. Cao, L. Wang, X. Chi, W. Gao, L.W. Wang, J. Comput. Phys. 251 (2013) 102–115.
[76] H. Wu, H. Yu, Z. Yang, X. Hou, X. Su, S. Pan, K.R. Poeppelmeier, J.M. Rondinelli, J. Am. Chem. Soc. 135 (2013) 4215–4218.
[77] B. Zhang, E. Tikhonov, C. Xie, Z. Yang, S. Pan, Angew. Chem. 131 (2019).
[78] C. Lee, W. Yang, R.G. Parr, Phys. Rev. B 37 (1988) 785–789.
[79] A.D. Becke, J. Chem. Phys. 38 (1988) 3098–3100.
[80] L.E. Roy, P.J. Hay, R.L. Martin, J. Chem. Theor. Comput. 4 (2008) 1029–1031.
[81] M.J. Frisch, G.W. Trucks, H.B. Schlegel, G.E. Scuseria, M.A. Robb, A.R. Cheeseman, G. Scalmani, V. Barone, B. Mennucci, G.A. Petersson, H. Nakatsuji, M. Caricato, X. Li, H.P. Hratchian, A.F. Izmaylov, J. Bloino, G. Zheng, J.L. Sonnenberg, M. Hada, M. Ehara, K. Toyota, R. Fukuda, J. Hasegawa, M. Ishida, T. Nakajima, Y. Honda, O. Kitao, H. Vreven, T. Nakai, J.A. Montgomery, J.E. Peralta Jr., F. Ogliaro, M. Bearpark, J.J. Heyd, E. Brothers, K.N. Kudin, V.N. Staroverov, T. Keith, R. Kobayashi, J. Normand, K. Raghavachari, A. Rendell, J.C. Burant, S.S. Iyengar, J. Tomasi, M. Cossi, N. Rega, J.M. Millam, M. Klene, J.E. Knox, J.B. Cross, V. Bakken, C. Adamo, J. Jaramillo, R. Gomperts, R.E. Stratmann, O. Yazyev, A.J. Austin, R. Cammi, C. Pomelli, J.W. Ochterski, R.L. Martin, K. Morokuma, V.G. Zakrzewski, G.A. Voth, P. Salvador, J.J. Dannenberg, S. Dapprich, A.D. Daniels, O. Farkas, J.B. Foresman, J.V. Ortiz, J. Cioslowski, D.X. Fox, Gaussian 09, Revision E.01, Gaussian, Inc., Wallingford CT, 2013.
[82] S.P. Guo, Y. Chi, H.G. Xue, Angew. Chem. Int. Ed. Engl. 57 (2018) 11540–11543.